ADITUM
Enrich your Research

Molecular Biology and Biochemistry

Research Article

Synovial Fluid Proteomics and Serum Metabolomics Reveal Molecular and Metabolic Changes in Osteoarthritis

Vishal Chandra[1], (Mohd.) Tashfeen Ashraf[2], Pramod Yadav[1,3*], Vikas Raghuvanshi[1,4],
[1]School of Life Sciences and Biotechnology, Chhatrapati Shahu Ji Maharaj University Kanpur, Uttar Pradesh, India,
[2]School of Biotechnology, Gautam Buddha University, Greater Noida, India,
[3]Amity Institute of Neuropsychology and Neurosciences, Amity University Uttar Pradesh, India, Orcid Scopus profile
[4]Madurai Kamaraj University, Tamil Nadu, India, Orcid vikashraghuvanshi2017

Article Info

Received: November 14, 2023
Accepted: November 22, 2023
Published: November 29, 2023

***Corresponding author:** Pramod Yadav, Department of AFAF, Amity University Uttar Pradesh, Noida Campus, 201313, India.

Citation: Yadav P, Chandra V, Ashraf T, Raghuvanshi V, (2023). "Synovial Fluid Proteomics and Serum Metabolomics Reveal Molecular and Metabolic Changes in Osteoarthritis". Molecular Biology and Biochemistry 1(1); DOI: http;//doi.org/08.2023/1.001.

Abstract:

Background: Osteoarthritis (OA) is a common joint disorder with a complex and multifactorial pathogenesis. Proteomics analysis using two-dimensional gel electrophoresis (2DE) and mass spectrometry (MS) enables high-throughput identification of differentially expressed proteins related to OA. However, the etiology, pathophysiology, and early diagnostic markers of OA are still poorly understood. *Methods:* Synovial fluid protein biomarkers were compared between OA patients and healthy controls. It was fractionated using DEAE cellulose and Sephadex G-200 columns, followed by SDS–PAGE and 2D-PAGE for visualization and identification. Mass spectrometry and Mascot were used for protein analysis, and serum metabolite profiles were also investigated using 1D 1H CPMG NMR spectra. Multivariate data analysis, including PCA and PLS-DA, was performed to detect metabolic differences between groups. *Results:* Proteomics analysis revealed differential expression of synovial fluid proteins, such as serine protease inhibitors, complement components, and apolipoproteins, which may be involved in inflammation and cartilage breakdown. Additionally, serum metabolite profiles differed significantly between OA patients and controls, involving amino acid, lipid, glucose, and energy metabolism. The pathway analysis indicated disruption of the metabolic pathways associated with these metabolites. *Conclusions:* This study provides insights into the molecular and metabolic changes in OA. Protein biomarkers and serum metabolite alterations enhance the understanding of OA pathogenesis and offer potential opportunities for early diagnosis and disease management. Further validation and translation of these findings into clinical applications are needed for improved OA detection and intervention strategies.

Keywords: Metabolomics, Mass spectrometry of synovial fluid, Biomarkers, Joint disease, Cartilage degeneration

Highlights:

- Serum metabolite profiles reveal metabolic alterations in OA patients.
- Pathway analysis shows disrupted metabolic pathways in OA patients.
- Protein biomarkers and metabolites enhance the understanding of OA pathogenesis.
- Potential diagnostic and prognostic markers for OA detection and management.

1. Introduction:

Osteoarthritis (OA) is a degenerative joint disease that affects the articular

cartilage, and its characteristics are increased friction, wear between bones, pain, swelling, stiffness and reduced mobility (1). Among these, pain is a common symptom of OA, but its origin is unclear since cartilage lacks nociceptors. Morning stiffness is another symptom, but it lasts less than 30 minutes, and patients may also experience joint instability or locking (2,3). According to the WHO, OA is expected to be the fourth leading cause of knee disability by 2024 (4). Globally, more than 100 million people suffer from OA, and it has a higher prevalence in women than men (5). The prevalence of knee OA increases with age and varies across regions, ranging from 7.5% in China (6) to 25% in northern Pakistan (7). In India, OA is the second most prevalent rheumatologic problem, with a prevalence of 22% to 39%, and affects 60.6% of the urban population and 5.78% of the rural population (8). Among people aged 65 years and above, OA accounts for 50% of all disability diseases (9). The pathogenesis of OA is complex and multifactorial, involving the interaction of cartilage, subchondral bone, periosteum, joint capsule, and synovial fluid (10). Physical examination is essential for diagnosis, and plain radiography can confirm OA in some cases, but advanced imaging techniques such as magnetic resonance imaging (MRI) are required for accurate diagnosis, especially if meniscal injury is suspected. However, these techniques are not affordable for many patients, resulting in underdiagnosis of OA. Despite considerable progress in OA research, its pathogenesis, etiology and progression remain poorly understood. Studies have reported abnormalities in the immune response and immune cells of OA patients, such as altered T-cell subsets. These abnormalities may play a role in the pathogenesis of OA and modulate the inflammatory response in the synovial membrane (SM), leading to cartilage degradation (11). Despite extensive research with multiple approaches, our understanding of OA etiology and pathophysiology and our ability to diagnose it at an early stage are limited [(2). The present study was undertaken to investigate the comparative analysis of protein biomarkers occurring in the synovial fluid of patients and healthy controls.

2. Methodology:

2.1. Inclusion and exclusion criteria of control and subject

We selected control subjects free of any clinical or radiological signs of joint disease, comorbidities, obesity, hypersensitivity, or cardiovascular disease. We used the Kellgren and Lawrence (K-L) score, the WOMAC score, the VAS score, and the American College of Rheumatology (ACR) classification to screen and evaluate OA patients. Only patients who met six or more criteria were included. Patients had knee pain (*asymmetrical*) lasting more than six months, stiffness (*less than 30 minutes*), swelling, cripitus, tenderness on the medical side of the joint, X-ray (*Grade II-78 and Grade III-22*), normal ligament stability, decreased motion, duration of symptoms (*3.3±1.49 years*), range of movements (*0-140/42± 20.2*), VAS pain on movement (*4.7±1.4 cm*) and WOMAC score of patients (*difficulty 31.0±8.1; pain 9.2±2.2; stiffness 4.2±1.3 and total 44.2±9.8*). We excluded patients with infectious diseases such as diabetes mellitus, hypertension, thyroid dysfunction, neurological disorders, cancer, or other forms of arthritis. We also excluded patients with early OA *(<2 years from symptom onset*). The current study was approved by the Institutional Ethical Committee (*CSJMU/BSBT/BT/EC-20*), and all participants provided written informed consent.

2.2. Synovial fluid protein analysis

Synovial fluid was obtained from patients and healthy controls by an orthopedic doctor and diluted with 50 mM Tris-HCl buffer (pH 8). The diluted samples were stored at 4°C and applied to a DEAE cellulose column with a linear gradient of 0-500 mM NaCl (250 ml) at a flow rate of 84 ml/h. The fractions were collected and reapplied to a Sephadex G-200 column equilibrated with Tris-Cl buffer (50 mM and pH 7.4) and NaCl (100 mM) at a 45 ml/h flow rate. The eluted proteins were precipitated with ammonium sulfate, dissolved in a buffer with protease inhibitors, and used for SDS–PAGE and 2D-PAGE [13–16]. For the first dimension in 2D-PAGE, the protein concentration was determined by the Bradford method. Then, 200 µg of protein was mixed with 5 µl of 10% SDS and 5.3 µl of 1 M DTT, boiled at 100°C for 5 minutes, and placed on ice. Then, 100-120 µl of rehydration buffer (with 0.5 g of total protein extraction buffer, 0.5 ml of total protein extraction diluent, 50 µl of DTT, 100 µl of protease inhibitors, and 0.2% ampholytes) was added and loaded onto an IPG strip for active rehydration overnight. After 11-16 hours of active rehydration, the strip was removed, wiped off with tissue paper, and placed on the power pack with the correct orientation of electrodes (+/-). The strips were transferred to the top of 12% acrylamide denaturing gels for the second dimension. For silver staining, the gels were washed in water overnight, dehydrated with 50% ethanol three times, sensitized for 1 minute in sodium thiosulfate (0.02%), washed two times in water, impregnated in silver nitrate (0.2%) for 20 minutes, washed with distilled water for one minute, developed with 6% sodium carbonate under light with constant stirring and formaldehyde until the desired color intensity was achieved, washed with distilled water, terminated by adding 5% methanol and 7% acetic acid, and stored in 50% ethanol. For Coomassie blue staining, the gels were stained overnight with a solution containing 0.125% Coomassie blue R250, 50% methanol and 10% acetic acid, destained with the same solution without Coomassie blue R250, and stored in a solution containing 7% methanol and 10% acetic acid.

2.3. MS/MS and data analysis

Protein bands were in-gel digested with trypsin (modified sequencing grade; Promega, USA) according to the reported protocol (17). The peptides were extracted, dried, desalted using ZipTip (Millipore, USA), and identified by nano-MS/MS. The peptides were reconstituted in 0.1% formic acid and subjected to LC–MS (Nano Advance, Bruker, Germany) and captive spray-Maxis-HD qTOF (Bruker, Germany) with high sensitivity and mass accuracy. The peptides were enriched in a nanotrap column (Bruker Magic C18AQ, particle size-5 µm, pore size-200 Å), separated on an analytical column (Bruker Magic C18AQ, 0.1 x 150 mm, 3 µm particle size and 200 Å pore size) at a flow rate of 800 nl/min and eluted using a linear gradient of 5-45% acetonitrile over 135 min (18). The MS scan was performed in the 400-1400 m/z range, followed by an MS/MS scan of the six most intense precursor ions from the survey scan. Peak graphs were obtained by Otof control (version 24.8) with the help of the Hystar postprocessing program and submitted to Protein Scape software

(Bruker, Germany), which uses Mascot (2.4.1 Matrix Science, UK). Mascot MS/MS ion search criteria were as follows: taxonomy Homo sapiens, trypsin digestion, allowing up to one missed cleavage, variable modification oxidation of methionine, fixed modification-cysteine as carboxyamidomethylation or propionamide, peptide tolerance of 50 ppm, and MS/MS tolerance of 0.05 Da. The "ion score cut-off" was set at 15 manually to eliminate the matches of lowest quality. To ensure the validity of the results, both protein and peptide identifications were subjected to a 1% FDR threshold [16].

2.4. Serum metabolite analysis

Serum samples were prepared by centrifuging clotted blood at 1200 rpm for 20 min at -4°C, aliquoting the supernatant, and storing it at -20°C. Prior to NMR analysis, serum samples were thawed, centrifuged at 10,000 rpm for 5 min to eliminate precipitates, and mixed with an equal volume of 0.9% saline sodium phosphate buffer (20 mM, pH 7.4) prepared in D_2O [19]. A coaxial insert containing 0.1% TSP (Sigma–Aldrich, Rhode Island, USA) in D_2O was used as an external standard reference for metabolite quantification. NMR spectra were acquired at 298 K on a Bruker Biospin Avance-III 800 MHz NMR spectrometer. Transverse relaxation edited CPMG spectra ID 1H NMR spectra [20] were recorded using the standard Bruker's pulse program library sequence (cpmgpr ID) with water peak presaturation during the RD of 5 s. Each spectrum had 128 scans and a total spin–spin relaxation time of 60 ms. FIDs were zero filled, Fourier transformed to 64 K data points, and manually phase and baseline corrected using Topspin-2.1. FIDs were processed with a 0.3 Hz line broadening and a sine-bell anodization prior to FT. The methyl peak of L-lactate (δ = 1.33 ppm) served as the internal reference for chemical shifts. Spectra were visually examined and analysed multivariate to detect the changes in metabolic profiles. Chemical shifts were assigned by comparing them with the shifts available from MetaboMiner25 [21] and Chenomx (NMR suite, v8.1, Chenomx Inc., Edmonton, Canada). The assigned resonances were validated using *(a)* assigned resonances in 2D spectra for unambiguous assignment and *(b)* previously reported NMR assignments of metabolites, data obtained from the BMRB database and HMDB [22–24]. 2D 1H-1H TOCSY and 1H-13C HSQC NMR spectra were also acquired for some of the serum samples using the parameters described previously [25].

3. Results:

3.1. Protein expression analysis by 2D-PAGE and MS/MS

The protein spots from the OA profile digested with trypsin were expunged from the 2D gel and analysed by MALDI-MS/MS. Many peptides and proteins were identified by searching the MascotTM database (see Fig. 1), and proteins were further classified according to the pathways in which they have major roles (see Annexture 2). Annex 1 shows 29 differentially expressed proteins with a score of more than 15. No disease duration-dependent difference in the expression profile was observed. Mass spectrometric analysis indicated changes in the abundance of complement components C3 and C4b and the immunoglobulin constant region. These proteins may play a role in OA pathogenesis; however, no direct disease-specific proteins were detected in this study.

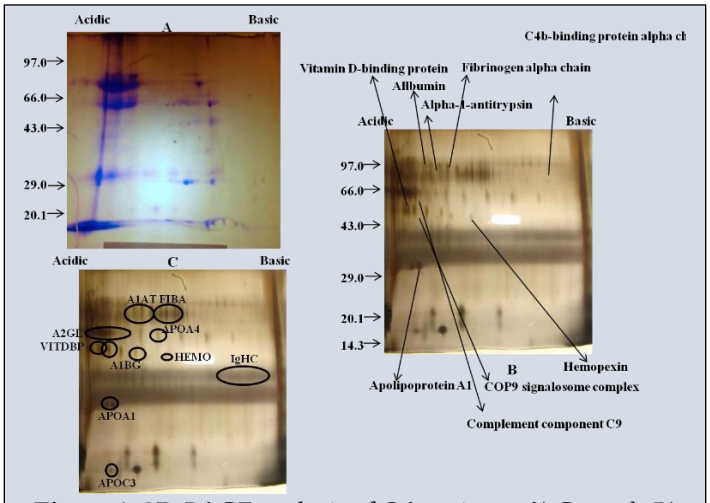

Figure 1. 2D-PAGE analysis of OA patients. *A)* Control; *B) and C)* OA patient profiles.

3.2. Serum metabolite expression analysis by 1D 1H CPMG NMR

The spectra (Fig. 3) displayed 1H NMR signals mainly from small metabolites with intense signals from lipoproteins, phospholipids, unsaturated lipids, choline metabolites, N-acetyl glycoproteins, glucose, lactate and amino acids. No major differences between the OA and control groups were observed by visual comparison. Hence, multivariate data analysis was performed on the NMR spectra to reveal the serum metabolic alterations caused by OA. The serum metabolic patterns of 10 grade II-III OA patients and sex-matched normal controls were analysed. The study subjects were selected to reduce the confounding variables (see Annexure 3). Fig. 3 shows that the OA group was clearly discriminated from the control group along the PC1 direction, indicating distinct characteristics of OA serum. This method also detected outliers outside the 95% confidence region of the PCA model. We then applied the supervised clustering method PLS-DA to examine the subtle metabolic variations among the groups. The quality of each model was assessed by the parameters R2 and Q2, which are shown in the respective score plots in Figure 3(B). The model quality parameters R2 and Q2 were significantly high (R2, Q2 > 0.7), indicating satisfactory fit and good predictive power of the PLS-DA models (constructed from CPMG spectra). The PLS-DA score plots also showed that the OA and control groups were well clustered and separated, reflecting significant differences in the biochemical composition profiles of serum metabolites in OA patients and normal controls. The metabolites responsible for the discrimination were identified using the VIP and $p < 0.05$ criteria. We identified 16 metabolites that were significantly perturbed in OA serum (VIP score ≥ 1) (see Fig 3 or Annexture 3).

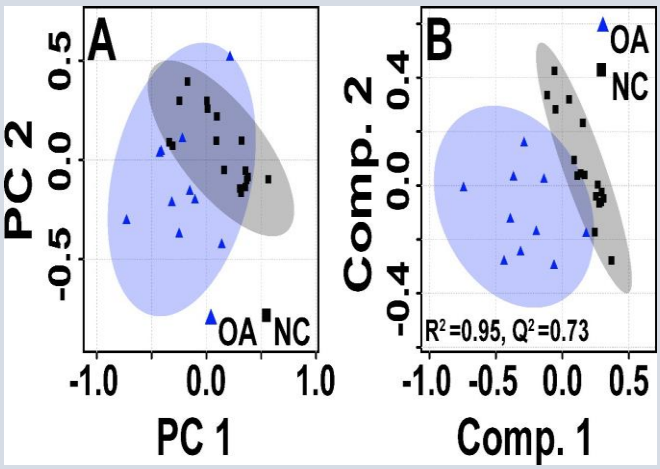

Figure 2. 2D-PCA. (A) Partial least square discriminant analysis (PLS-DA) (B) score plots.

[CPMG spectra showing clear statistical separation between OA (represented by blue triangles) and normal control (NC) samples (represented by black squares). Each circle and triangle represent one subject. The validation parameters (R2 and Q2) corresponding to the PLS-DA model are also displayed in their score plots]

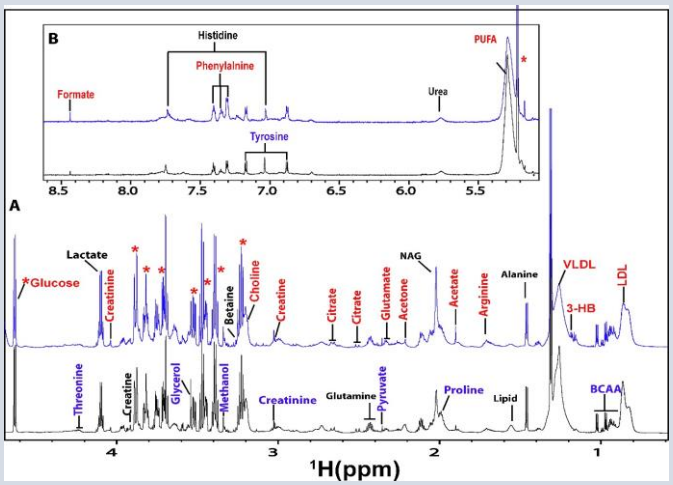

Figure 3. Stack plot of cumulative 1D 1H CPMG NMR spectra (A) from δ4.6–δ0.7 and (B) δ8.5–δ5.1 ppm) obtained for sera of OA patients (red) and normal controls (blue).

3.2.1. Heatmaps

Fig. 4 shows the heatmaps for different metabolites that distinguish the OA group from the control group (upregulated and downregulated metabolites are shown in red and cyan, respectively). Consistent with our serological data, we found high serum creatinine and a low HDL/LDL ratio in OA by NMR analysis. OA is typically associated with dyslipidemia and has high serum creatinine and low uric acid, as identified by serological analysis. Using a nonparametric Mann–Whitney test, we quantified the differential abundance of metabolites and found that most of them were statistically significant ($p < 0.05$). The discriminating metabolic features were predominantly associated with lipid, amino acid, glucose and energy metabolism.

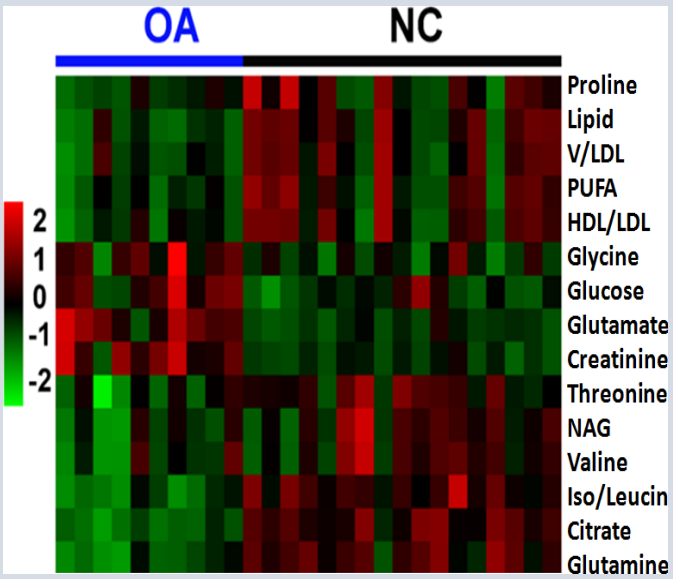

Figure 4. Heatmaps depicting z scores of 16 metabolites of OA patients and normal controls.

3.2.2 zROC curves:

The area under the ROC curve reflects the discriminatory ability (0.5 indicates no discrimination; 1 indicates perfect discrimination). The AUC values ranged from 0.95 to 0.55 (see Fig. 5), indicating that these metabolites could be potential biomarkers for the clinical evaluation and surveillance of such patients. Figure 5 depicts representative ROC curves for some of the serum metabolites that exhibited significant changes in OA patients and their corresponding box plots (from the univariate analysis).

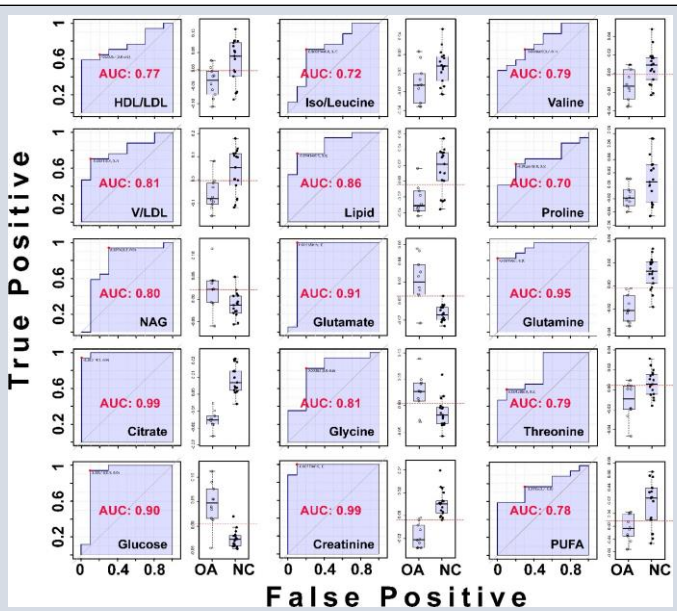

Figure 5. ROC curves along with their respective box plots.

[Respective box plots of the significant metabolites that decreased or increased in the OA patients compared to the control group derived from the CPMG 1H NMR spectra. Boxes denote interquartile ranges, lines denote medians, and whiskers denote 10th and 90th percentiles.]

3.2.3 Metabolic pathway by ORA

Fig. 6 summarizes the pathway analysis and MSEA in MetaboAnalyst results. Five important metabolic pathways (protein biosynthesis, amino acid metabolism, glucose-energy metabolism) were found to be disturbed. The metabolic pathways associated with the identified combinations of metabolites are biased due to limited metabolites detected by NMR in the serum.

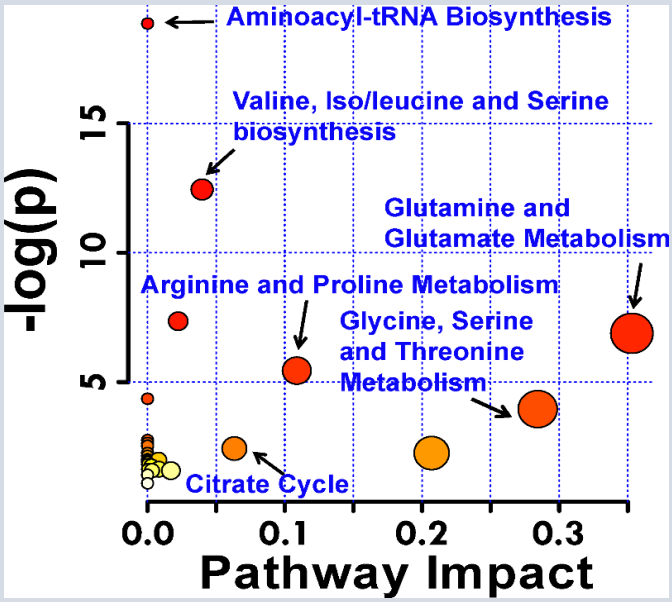

Figure 6. A diagram of a pathway impact by ORA.

[The analysis was performed by using a pathway library restricted to Homo sapiens, and p values for ORA represent hypergeometric tests. Test p value (vertical axis, colour intensity) and impact factor (horizontal axis, circle size)].

4. Discussion:

4.1. Proteomics profile analysis by mass spectrometry

This study proposed that some proteins were overexpressed in OA patients, but none of these proteins were directly implicated in the pathophysiology of the disease (see Annexure 3). We identified several proteins, such as serine protease inhibitors, high levels of ATIII, and proteins related to lipid transport or protein binding, such as apolipoproteins, immunoglobulins, transmembrane proteins and transcriptional proteins. These proteins are involved in cartilage degradation or protein synthesis. Olsen et al. reported that the levels of APO-A1 in the synovial fluid of OA patients are higher due to diffusion and production by chondrocytes and FLSs (26). Our results confirmed the role of APO-A1 in inflammation with increased expression of fibrinogen protein in OA and confirmed that these proteins can trigger TLR-4-dependent macrophage production of inflammatory cytokines and growth factors. This study reports high expression and activation of complement in OA joints. It also identified the proinflammatory complement components C3, C4b, and C9. C9 components from MAC were aberrantly expressed in OA, and C3 and C4b were higher in the early stage of OA. Hemopexin (HPX) is an acute phase protein that suppresses the adhesion of leukocytes and the release of cytokines from macrophages. Its high level suggests its role in OA. We also identified proteins involved in extracellular matrix, cartilage, and bone metabolism. Rab5 GDP/GTP exchange factor expression supports the role of the Ras superfamily in OA progression.

4.2. Metabolite analysis by NMR

The results of this study indicate that early metabolic changes in OA can be detected in serum by NMR. According to a study, degenerative joint disease can affect the synovium, as it becomes hypoxic (27). This is also observed due to increased lactate concentration. This study found an increased creatinine concentration that indicates altered metabolism in early OA. Similar results have been reported for the serum metabolite profile in a sheep model of OA (28). We observed increased glutamine and glutamate concentrations in the serum of OA patients. Glutamine confers chondrocyte resistance to heat stress and NO-mediated apoptosis (29). Hence, glutamine elevation may reflect chondrocyte adaptation to various stressors during disease progression. Choline augmentation might indicate lipid catabolism from articular cartilage and leakage of its products into the bloodstream due to synovial membrane permeability enhancement. Alternatively, increased choline could result from the breakdown of Hoffa's pad or phospholipids in the joint (30). We also found reduced leucine and histidine in the serum of OA patients. Comparison of spectral profiles of controls and patients reveals that cartilage breakdown continues with increased glycerol and hydroxybutyrate. Glycerol synthesis indicates triglyceride degradation in various tissues. Moreover, the decreased HDL/LDL ratio and PUFAs reflect the impact of free radical generation through lipid peroxidation, leading to high oxidative stress and inflammation (31).

5. Conclusion:

Proteomics analysis using 2D-PAGE coupled with mass spectrometry revealed differentially expressed proteins involved in inflammation, oxidative stress, and the immune response, suggesting a complex interplay of factors in OA pathogenesis. NMR-based metabolomics analysis identified altered metabolic patterns in the serum of OA patients, indicating hypoxia, inflammation, and lipid metabolism disruption. Increased lactate and creatinine levels suggest tissue hypoxia and muscle breakdown near the affected joint. Alterations in amino acids, lipoproteins, and glucose-energy metabolism indicate disrupted metabolic pathways in OA patients. The integration of proteomics and metabolomics data provided a comprehensive view of the disease, highlighting potential targets for further investigation. The identified proteins and metabolites could serve as candidates for future diagnostic or prognostic biomarkers for OA. Further studies are needed to validate these findings and improve our understanding of OA pathophysiology and early detection.

Annexture 1. Proteins identified from OA samples along with their structural and functional characteristics.

Accession	Protein	Modifications/function	pI	MW [kDa]	#Alt. Protein	Scores	SC [%]	RMS90 [ppm]
AACT_HUMAN	Alpha-l-antichymotrypsin sapiens	Oxidation (inhibitor)	5.3	47.6	1	339.6 (M:339.6)	16.5	40.27
ANT3_HUMAN	Antithrombin-III	Nonvitamin K-dependent protease	6.3	52.6	1	56.2 (M:56.2)	2.6	39.85
AIBG_HUMAN	Alpha-lB-glycoprotein	Upregulated in adenocarcinoma-unknown function	5.6	54.2	1	21.1 (M:21.1)	1.6	41.8
APOA1_HUMAN	Apolipoprotein A-I	Cholesterol metabolism	5.6	30.8	1	172 (M:172.0)	22.5	23.66
AIBG_HUMAN	Alpha-lB-glycoprotein	Carbamidomethyl/Upregulated in adenocarcinoma-unknown function	5.6	54.2	1	705.7 (M:705.7)	38.2	9.87
CO9_HUMAN	Complement component C9 C4b-binding protein alpha	Complement cascade	5.4	63.1	1	50.3 (M:50.3)	2.1	39.23
C4BPA_HUMAN	chain	Complement cascade	7.2	67	1	15.1 (M:15.1)	1.8	40.78
CO3_HUMAN	Complement C3	Oxidation/Complement cascade	6	187	1	313.7 (M:313.7)	4.1	24.23
CSN2_HUMAN	COP9 signalosome complex subunit 2	Ubiquitin regulator	5.4	51.6	1	17.0 (M:17.0)	2.3	763.59
EFCB7HUMAN	EF-hand calcium-binding domain-containing protein 7	Carbamidomethy Ucytoplasmic calcium sensor	6	71.9	1	31.6 (M:31.6)	1.6	44.1
FIBA_HUMAN	Fibrinogen alpha chain	Act as DAMPs	5.7	94.9	1	82.0 (M:82.0)	3.1	40.02
HBB_HUMAN	Hemoglobin subunit beta	Oxidation/blood pigment	6.7	16	5	187.8 (M:187.8)	28.6	14.73
HEMO_HUMAN	Hemopexin	Carbamidomethyl, Oxidation/inflammation induced acute phase protein	6.5	51.6	1	381.8 (M:381.8)	32.7	39.92
HRG_HUMAN	Histidine-rich glycoprotein	Carbamidomethyl/roles in immunity, coagulation	7.1	59.5	1	169.3 (M:169.3)	10.1	39.27
IGHA1_HUMAN	Ig alpha-1 chain C region	Carbamidomethyl/immunity	6.1	37.6	2	235.4 (M:235.4)	21.8	40.36
KV311_HUMAN	Ig kappa chain V-III region IARC/BL41	immunity	6.2	14.1	1	80.6 (M:80.6)	12.5	23.77

IGHG1_HUMAN	Ig gamma-1 chain C region	Carbamidomethyl/immunity	8.5	36.1	2	61.5 (M:61.5)	7.9	23.62
LV_l02_HUMAN	Ig lambda chain V-I region HA	Immunity	9.1	11.9	2	56.3 (M:56.3)	18.8	24.64
TRFM_HUMAN	Melanotransferrin	Carbamidomethyl/Role in melanoma cell proliferation and tumorigenesis	5.6	80.2	1	41.6 (M:41.6)	1.8	780.36
OSGI2_HUMAN	Oxidative stress-induced growth inhibitor 2	Oxidation/apoptotic regulator	7	56.6	1	16.2 (M:16.2)	1.6	1076.69
THRB_HUMAN	Prothrombin	Blood clotting	5.6	70	1	31.5 (M:31.5)	1.6	7.97
KS6A3_HUMAN	Ribosomal protein S6 kinase alpha 3	Oxidation/Mediates cell survival	6.4	83.7	1	17.4 (M:17.4)	1.2	31.89
RMD2_HUMAN	Regulator of microtubule dynamics protein 2	Role in signaling	6.1	47.4	1	16.5 (M:16.5)	4.6	4.1
RABXS_HUMAN	Rab5 GDP/GTP exchange factor	Involved in signaling	6.4	79.3	1	17.2 (M:17.2)	1.8	632.58
RB27B_HUMAN	Ras-related protein Rab-27B	Involved in vesicular fusion and trafficking	5.4	24.6	1	15.1 (M:15.1)	5	774.92
ARRS_HUMAN	S-arrestin	Role in retinal photoreceptorcells	6.1	45.1	1	16.4 (M:16.4)	3.2	48.05
TRFE_HUMAN	Serotransferrin	Oxidation/uptake of transferring bound iron	6.8	77	1	4161.6 (M:4161.6)	63.8	10.29
TMM78_HUMAN	Transmembrane protein 78	-	4.9	15.2	1	18.1 (M:18.1)	5.9	1229.9
VTDB_HUMAN	Vitamin D binding protein	Bone metabolism	5.4	52.9	1	19.5 (M:19.5)	2.3	10.76

[(PE: protein existence, SV: sequence version, MW [kDa], pI: isoelectric point, Score: Mascot score, SC: sequence coverage, RMS90 [ppm]: root mean square (RMS.)]

Annexture 2. List of OA disease-associated proteins and their classification.

Serine protease inhibitors/signalling proteins	**Bone metabolism/ pathway regulators**	**Inflammation and immunologic cascade**	**Oxidative stress**	**Cholesterol metabolism**
Alpha 1	Vitamin D binding	Alpha 1B glycoprotein	Hemopexin	Apolipoprotein A
antichymotrypsin	protein	Apolipoprotein A1	Transmembrane	EF hand
Antithrombin III	Zinc finger and BTB	Fibrinogen alpha chain	protein78	calcium binding domain
Hemopexin	domain protein 45	Rab5 GDP/GTP exchange	Oxidative	
Prothrombin		factor	stress-induced	
Serotransferrin		S-arrestin	growth	
Melanotransferrin		Complement C3	inhibitor 2	
COP9 signalosome		Complement component C9		
complex subunit 2		C4 binding protein α chain		

Annexture 3. List of OA disease-associated proteins and their classification.

Serine protease inhibitors/signalling proteins	Bone metabolism/ pathway regulators	Inflammation and immunologic cascade	Oxidative stress	Cholesterol metabolism
Alpha 1	Vitamin D binding	Alpha 1B glycoprotein	Hemopexin	Apolipoprotein A
antichymotrypsin	protein	Apolipoprotein A1	Transmembrane	EF hand
Antithrombin III	Zinc finger and BTB	Fibrinogen alpha chain	protein78	calcium binding domain
Hemopexin	domain protein 45	Rab5 GDP/GTP exchange	Oxidative	
Prothrombin		factor	stress-induced	
Serotransferrin		S-arrestin	growth	
Melanotransferrin		Complement C3	inhibitor 2	
COP9 signalosome		Complement component C9		
complex subunit 2		C4 binding protein α chain		

[The terms 'up' and 'down' denote elevated and reduced metabolite levels in OA patients compared to normal controls. (AUC: Area under curve (receiver operating characteristic curve), VIP: Variable importance in projection (for quantitative estimation of discriminatory power of each individual feature).

Abbreviation:

OA	-	Osteoarthritis
MS	-	Mass Spectrometry
2DE	-	Two-Dimensional Gel Electrophoresis
SDS–PAGE	-	Sodium Dodecyl Sulfate–Polyacrylamide Gel Electrophoresis
NMR	-	Nuclear Magnetic Resonance
PCA	-	Principal Component Analysis
PLS-DA	-	Partial Least Squares-Discriminant Analysis
WHO	-	World Health Organization
K-L	-	Kellgren and Lawrence
WOMAC	-	Western Ontario and McMaster Universities Arthritis Index
VAS	-	Visual Analog Scale
ACR	-	American College of Rheumatology
DEAE	-	Diethylaminomethyl
SM	-	Synovial Membrane
MRI	-	Magnetic Resonance Imaging
RA	-	Rheumatoid Arthritis
VIP	-	Variable Importance in Projection
AUC	-	Area Under Curve
FDR	-	False Discovery Rate
HDL	-	High-Density Lipoproteins
LDL	-	Low-Density Lipoproteins
PUFA	-	Polyunsaturated Fatty Acids
ORA	-	Over-Representation Analysis
DAMPs	-	Damage-Associated Molecular Patterns
TLR-4	-	Toll-like Receptor 4

Declaration(s):

Competing interests: The authors report no conflicts of interest.

Author 1 declared no conflict of interest.
Author 2 declared no conflict of interest.
Author 3 declared no conflict of interest.
Author 4 declared no conflict of interest.

Funding: This research was unfunded by any public, commercial, or not-for-profit agencies.

Ethical Approval and Consent to Participate: The study adhered to the ethical standards of India and internationally, with approval from the Institutional Ethical Committee (CSJMU/BSBT/BT/EC-20) and written informed consent from all patients, including controls and OA subjects.

Guarantor: The article's full responsibility lies with PY, who is the corresponding author and the third author in the list.

Authors' contributions: Dr. VC was responsible for manuscript conceptualization, writing - original draft, ethical approvals, consent, and sample collection. VR participated in writing - review & editing. PY contributed to manuscript writing, formatting, revision and communication with all authors. Dr. TA supervised all authors and wrote, reviewed and edited the final manuscript.

Acknowledgements: The authors thank the Institute of Biosciences and Biotechnology, Chhatrapati Shahu Ji Maharaj University, Kanpur - 208024, India, for providing the laboratory facilities and the Department of the Community Health Centre, Ganesh Shankar Vidyarthi Memorial Medical College (GSVM) Medical College, Kanpur – 208002, India, for recruiting the controls and subjects.

Availability of data and materials: Data and materials are available upon request.

Consent for publication: All authors consented to manuscript publication.

References:

1. Hunter DJ, Bierma-Zeinstra S. Osteoarthritis. The Lancet 2019;393:1745–59..
2. Sibbritt D, Sundberg T, Ward L, Broom A, Frawley J, Bayes J, et al. What is the healthcare utilisation and out-of-pocket expenditure associated with osteoarthritis? A cross-sectional study. BMJ Open 2022;12..
3. Altman R, Asch E, Bloch D, Bole G, Borenstein D, Brandt K, et al. Development of criteria for the classification and reporting of osteoarthritis. Classification of osteoarthritis of the knee. Diagnostic and Therapeutic Criteria Committee of the American Rheumatism Association. Arthritis Rheum 1986;29:1039–49.
4. WHO reveals leading causes of death and disability worldwide: 2000-2019 n.d. https://www.who.int/news/item/09-12-2020-who-reveals-leading-causes-of-death-and-disability-worldwide-2000-2019 (accessed July 24, 2023).
5. Thati S. Gender Differences in Osteoarthritis of Knee: An Indian Perspective. J Midlife Health 2021;12:16.
6. Xiang YJ, Dai SM. Prevalence of rheumatic diseases and disability in China. Rheumatol Int 2009;29:481–90
7. Farooqi A, Gibson T. Prevalence of the major rheumatic disorders in the adult population of north Pakistan. Br J Rheumatol 1998;37:491–5.
8. [Joshi VL, Chopra A. Is there an urban-rural divide? Population surveys of rheumatic musculoskeletal disorders in the Pune Region of India using the COPCORD Bhigwan model. Journal of Rheumatology 2009;36:614–22.
9. Biehl M, Damm P, Trepczynski A, Preiss S, Salzmann GM. Towards planning of osteotomy around the knee with quantitative inclusion of the adduction moment: a biomechanical approach. J Exp Orthop 2021;8:39.
10. Chandnani VP, Ho C, Chu P, Trudell D, Resnick D. Knee hyaline cartilage evaluated with MR imaging: a cadaveric study involving multiple imaging sequences and intraarticular injection of gadolinium and saline solution. Radiology 1991;178:557–61.
11. Qiu G, Zhong S, Xie J, Feng H, Sun S, Gao C, et al. Expanded CD1c+CD163+ DC3 Population in Synovial Tissues Is Associated with Disease Progression of Osteoarthritis. J Immunol Res 2022;2022.
12. Bhattacharjee M, Balakrishnan L, Renuse S, Advani J, Goel R, Sathe G, et al. Synovial fluid proteome in rheumatoid arthritis. Clin Proteomics 2016;13.
13. Chandra DrV, Ashraf Dr (Mohd.) T, Yadav P, Raghuvanshi MrV. Gene Expression Profiles of Knee Osteoarthritis Patients and Healthy Controls: A Microarray Analysis Study. Preprint -SSRN 2023..Yadav P. Challenges & Solutions for Recent Advancements in Multi-Drugs Resistance Tuberculosis: A Review. Microbiol Insights 2023;16:1–9.
14. Raghuvanshi V, Yadav P, Ali S. Interferon production by Viral, Bacterial & Yeast system: A comparative overview in 2023. Int Immunopharmacol 2023;120.
15. Rawat P, Bathla S, Baithalu R, Yadav ML, Kumar S, Ali SA, et al. Identification of potential protein biomarkers for early detection of pregnancy in cow urine using 2D DIGE and label free quantitation. Clin Proteomics 2016;13.
16. Habdous M, Vincent-Viry M, Visvikis S, Siest G. Rapid spectrophotometric method for serum glutathione S-transferases activity. Clinica Chimica Acta 2002;326:131–42.
17. Bathla S, Rawat P, Baithalu R, Yadav ML, Naru J, Tiwari A, et al. Profiling of urinary proteins in Karan Fries cows reveals more than 1550 proteins. J Proteomics 2015;127:193–201
18. [Dona AC, Jiménez B, Schafer H, Humpfer E, Spraul M, Lewis MR, et al. Precision high-throughput proton NMR spectroscopy of human urine, serum, and plasma for large-scale metabolic phenotyping. Anal Chem 2014;86:9887–94..
19. Tang H, Wang Y, Nicholson JK, Lindon JC. Use of relaxation-edited one-dimensional and two dimensional nuclear magnetic resonance spectroscopy to improve detection of small metabolites in blood plasma. Anal Biochem 2004;325:260–72.
20. Xia J, Bjorndahl TC, Tang P, Wishart DS. MetaboMiner--semi-automated identification of metabolites from 2D NMR spectra of complex biofluids. BMC Bioinformatics 2008;9.
21. Nicholson JK, Foxall PJD, Spraul M, Farrant RD, Lindon JC. 750 MHz 1H and 1H-13C NMR Spectroscopy of Human Blood Plasma. Anal Chem 1995;67:793–811.
22. Guleria A, Bajpai NK, Rawat A, Khetrapal CL, Prasad N, Kumar D. Metabolite characterisation in peritoneal dialysis effluent using high-resolution (1) H and (1) H-(13) C NMR spectroscopy. Magn Reson Chem 2014;52:475–9.
23. Wishart DS, Jewison T, Guo AC, Wilson M, Knox C, Liu Y, et al. HMDB 3.0--The Human Metabolome Database in 2013. Nucleic Acids Res 2013;41..
24. Guleria A, Misra DP, Rawat A, Dubey D, Khetrapal CL, Bacon P, et al. NMR-Based Serum Metabolomics Discriminates Takayasu Arteritis from Healthy Individuals: A Proof-of-Principle Study. J Proteome Res 2015;14:3372–81.
25. [Olsen AK, Sondergaard BC, Byrjalsen I, Tanko LB, Christiansen C, Müller A, et al. Anabolic and catabolic function of chondrocyte ex vivo is reflected by the metabolic processing of type II collagen. Osteoarthritis Cartilage 2007;15:335–42.
26. Rice D, McNair PJ, Dalbeth N. Effects of cryotherapy on arthrogenic muscle inhibition using an experimental model of knee swelling. Arthritis Care Res (Hoboken) 2009;61:78–83.
27. Maher AD, Coles C, White J, Bateman JF, Fuller ES, Burkhardt D, et al. 1H NMR spectroscopy of serum reveals unique metabolic fingerprints associated with subtypes of surgically induced osteoarthritis in sheep. J Proteome Res 2012;11:4261–8.
28. Tonomura H, Takahashi KA, Mazda O, Arai Y, Inoue A, Terauchi R, et al. Glutamine protects articular chondrocytes from heat stress and NO-induced apoptosis with HSP70 expression. Osteoarthritis Cartilage 2006;14:545–53.
29. Lacitignola L, Fanizzi FP, Francioso E, Crovace A. 1H NMR investigation of normal and osteo-arthritic synovial fluid in the horse. Vet Comp Orthop Traumatol 2008;21:85–8.
30. Yoshihara Y, Nakamura H, Obata K, Yamada H, Hayakawa T, Fujikawa K, et al. Matrix metalloproteinases and tissue inhibitors of metalloproteinases in synovial fluids from patients with rheumatoid arthritis or osteoarthritis. Ann Rheum Dis 2000;59:455–61.